DOI: 10.1021/ic100636j

Inorganic Chemistry
Article

Density Functional Theory Interpretation of the ^{1}H Photo-Chemically Induced Dynamic Nuclear Polarization Enhancements Characterizing Photoreduced Polyazaaromatic Ru(II) Coordination Complexes

Emilie Cauët,[†] Stuart Bogatko,[†] Epiphanie Mugeniwabagara,[‡] Luca Fusaro,[‡] Andrée Kirsch-De Mesmaeker,[§] Michel Luhmer,[‡] and Nathalie Vaeck*,[†]

[†]*Service de Chimie Quantique et Photophysique, CP 160/09,* [‡]*Laboratoire de Résonance Magnétique Nucléaire Haute Résolution, CP 160/08, and* [§]*Service de Chimie Organique et Photochimie, CP 160/08, Université Libre de Bruxelles, 50 Avenue F.D. Roosevelt, B-1050 Bruxelles, Belgium*

Received April 3, 2010

The unprotonated and protonated monoreduced forms of the polyazaaromatic Ru(II) coordination complexes $[Ru(tap)_3]^{2+}$ and $[Ru(tap)_2(phen)]^{2+}$ (tap = 1,4,5,8-tetraazaphenanthrene ; phen = 1,10-phenanthroline), that is, $[Ru(tap)_3]^{\bullet+}$, $[Ru(tap)_2(phen)]^{\bullet+}$, $[Ru(tap)_2(tap\text{-}H)]^{\bullet 2+}$, and $[Ru(tap)(tap\text{-}H)(phen)]^{\bullet 2+}$, were studied by Density Functional Theory (DFT). The electron spin density of these radical cations, the isotropic Fermi-contact, and the anisotropic dipolar contributions to the hyperfine coupling constants of the H nuclei were calculated in vacuo and using a continuum model for water solvation. For $[Ru(tap)_2(phen)]^{\bullet+}$, as well as for its protonated form, the DFT results show that the unpaired electron is not localized on the phen ligand. For both $[Ru(tap)_3]^{\bullet+}$ and $[Ru(tap)_2(phen)]^{\bullet+}$, they reveal high electron spin density in the vicinity of tap H-2 and tap H-7 (the H atoms in the ortho position of the tap non-chelating N atoms). These results are in full agreement with recent steady-state ^{1}H photo-Chemically Induced Dynamic Nuclear Polarization (photo-CIDNP) measurements. The DFT calculations performed for the protonated species also predict major ^{1}H photo-CIDNP enhancements at these positions. Interestingly, they indicate significantly different polarization for tap H-9,10, suggesting that the occurrence of a photoinduced electron transfer with protonation of the reduced species might be detected by high-precision photo-CIDNP experiments.

Introduction

$[Ru(tap)_3]^{2+}$ and $[Ru(tap)_2(phen)]^{2+}$ (tap = 1,4,5,8-tetraazaphenanthrene ; phen = 1,10-phenanthroline) (Chart 1) are known to photo-oxidize biomolecules such as the purine nucleobase guanine and the amino acids tyrosine and tryptophan.[1−3] It has also been demonstrated that these photo-oxidizing tap Ru(II) complexes give rise to the formation of covalent photoadducts[1,4] and, therefore, they are presently developed as potential photoactive drugs in gene therapy.[5,6]

Recently, some of us showed that the photoreaction of $[Ru(tap)_3]^{2+}$ and $[Ru(tap)_2(phen)]^{2+}$ with guanosine-5′-monophosphate (GMP) or *N*-acetyl-tyrosine (*N*-Ac-Tyr) give rise to ^{1}H photo-Chemically Induced Dynamic Nuclear Polarization (photo-CIDNP).[7] CIDNP refers to non-Boltzmann nuclear spin state distributions in the diamagnetic products of radical reactions and is detected by NMR (Nuclear Magnetic Resonance) spectroscopy as enhanced absorption or emission signals.[8−10] Photo-CIDNP has been extensively used to probe the surface structure of proteins, to study protein folding, and also to investigate recognition processes.[8,11−13]

*To whom correspondence should be addressed. E-mail: nvaeck@ulb.ac.be. Phone: +32 2 650 4728. Fax: +32 2 650 4232.

(1) Gicquel, E.; Boisdenghien, A.; Defrancq, E.; Moucheron, C.; Kirsch-De Mesmaeker, A. *Chem. Commun.* **2004**, 2764.
(2) Elias, B.; Kirsch-De Mesmaeker, A. *Coord. Chem. Rev.* **2006**, *250*, 1627.
(3) Herman, L.; Ghosh, S.; Defrancq, E.; Kirsch-De Mesmaeker, A. *J. Phys. Org. Chem.* **2008**, *21*, 670.
(4) Jacquet, L.; Kelly, J. M.; Kirsch-De Mesmaeker, A. *J. Chem. Soc., Chem Commun.* **1995**, 913.
(5) Deroo, S.; Le Gac, S.; Ghosh, S.; Villien, M.; Gerbaux, P.; Defrancq, E.; Moucheron, C.; Dumy, P.; Kirsch-De Mesmaeker, A. *Eur. J. Inorg. Chem.* **2009**, 524.
(6) Legac, S.; Rickling, S.; Gerbaux, P.; Defrancq, E.; Moucheron, C.; Kirsch-De Mesmaeker, A. *Angew. Chem.* **2009**, *48*, 1122.
(7) Perrier, S.; Mugeniwabagara, E.; Kirsch-De Mesmaeker, A.; Hore, P. J.; Luhmer, M. *J. Am. Chem. Soc.* **2009**, *131*, 12458.
(8) Kaptein, R. Photo-CIDNP Studies of Proteins. In *Biological Magnetic Resonance*; Berliner, L. J., Reubens, J., Eds.; Plenum Press: New York, 1982; Vol. *4*.
(9) Goez, M. Photo-CIDNP Spectroscopy. In *Annual Reports on NMR Spectroscopy*; Webb, G., Ed.; Academic Press: London, 2009; Vol. *66*.
(10) Kuhn, L. T.; Bargon, J. *Top. Curr. Chem.* **2007**, *276*, 125.
(11) Hore, P. J.; Broadhurst, R. W. *Prog. Nucl. Magn. Reson. Spectrosc.* **1993**, *25*, 345.
(12) Maeda, K.; Lyon, C. E.; Lopez, J. J.; Cemazar, M.; Dobson, C. M.; Hore, P. J. *J. Biomol. NMR* **2000**, *16*, 235.
(13) Mok, K. H.; Hore, P. J. *Methods* **2004**, *34*, 75.

Published on Web 08/06/2010

Chart 1. Structure and Numbering of the Ligands tap (top, left) and phen (top, right) and of the Ru(II) Complexes $[Ru(tap)_3]^{2+}$ (bottom, left) and $[Ru(tap)_2(phen)]^{2+}$ (bottom, right)

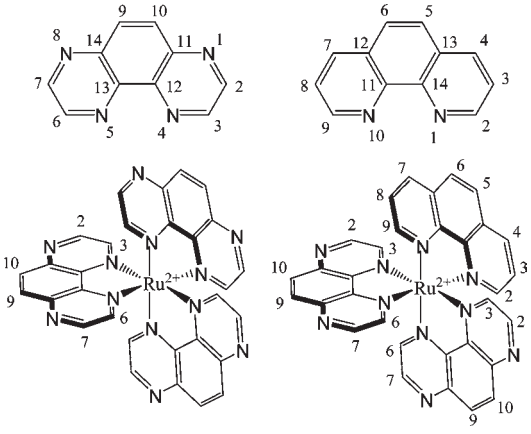

The radical pair mechanism is currently accepted as the most common origin of CIDNP in solution.[14,15] Accordingly, CIDNP can be observed for the nuclear spins that have a hyperfine interaction with an unpaired electron in transient radical pairs. For the systems under study, these radical pairs arise from the reductive quenching of metal-to-ligand charge-transfer triplet excited states (^{3}MLCT) of the Ru(II) complex by the biomolecule. Results of steady-state ^{1}H photo-CIDNP experiments showed no ^{1}H polarization for the phen ligand of $[Ru(tap)_2(phen)]^{2+}$ and, for both $[Ru(tap)_3]^{2+}$ and $[Ru(tap)_2(phen)]^{2+}$ complexes, a significant ^{1}H polarization enhancement for the H in the ortho position of the tap non-chelating N atoms (tap H-2 and H-7).[7] Straightforward interpretation of these results lead to the following conclusions: (i) in the monoreduced complex of $[Ru(tap)_2(phen)]^{2+}$, the unpaired electron is not localized on the phen ligand and (ii) the monoreduced complex of both $[Ru(tap)_3]^{2+}$ and $[Ru(tap)_2(phen)]^{2+}$ is characterized by a high unpaired electron density in the vicinity of positions 2 and 7 of the tap ligands. However, the magnitude of steady-state photo-CIDNP enhancements depends in an intricate way on various processes, among which paramagnetic relaxation,[7−10] and the interpretation of the experimental results must still be confirmed. Furthermore, it remains an open question whether or not a proton transfer at the level of a tap non-chelating N atom can accompany the electron transfer and affect the ^{1}H polarization pattern of the complexes. Therefore, Density Functional Theory (DFT) calculations were carried out for the unprotonated form of the monoreduced Ru(II) complexes, that is, $[Ru(tap)_3]^{\bullet+}$ and $[Ru(tap)_2(phen)]^{\bullet+}$, as well as for the corresponding protonated species, $[Ru(tap)_2(tap\text{-}H)]^{\bullet 2+}$ and $[Ru(tap)(tap\text{-}H)(phen)]^{\bullet 2+}$. The electron spin density and the isotropic Fermi-contact contribution to the hyperfine interactions of the ^{1}H nuclei were calculated and compared to the observed ^{1}H photo-CIDNP enhancements.[16,17] The anisotropic part of the hyperfine interactions was also computed and the effect of ^{1}H paramagnetic relaxation is discussed. The impact of the protonation on the ^{1}H polarization pattern is investigated.

Methods

The molecular structure and numbering of the Ru(II) complexes $[Ru(tap)_3]^{2+}$ and $[Ru(tap)_2(phen)]^{2+}$ and of the ligands tap and phen are shown in Chart 1. For $[Ru(tap)_2(tap\text{-}H)]^{\bullet 2+}$ and $[Ru(tap)(tap\text{-}H)(phen)]^{\bullet 2+}$, one tap ligand was replaced by a tap-H ligand in which one non-chelating N atom (N-1 or N-8) is protonated. The unrestricted DFT formalism was used for all the systems. This includes the spin polarization effects that have been shown to be important to describe correctly the isotropic hyperfine coupling constants.[18] All calculations were performed using the NWChem computational chemistry package.[19] As a first step, the geometries of the ground state of the low-spin Ru(II) ($4d^6$ valence configuration) complexes were optimized in vacuo using the B3LYP functional.[20,21] The 6-31G* basis set[22,23] was used for the C, N, and H atoms while the "Stuttgart RSC 1997 ECP"[24] relativistic effective core potential and associated basis set was employed to describe the Ru atom. This potential has been shown to allow an accurate description of the electronic and bonding properties of Ru complexes.[25−30] The structures obtained for the $[Ru(tap)_3]^{\bullet+}$ and $[Ru(tap)_2(phen)]^{\bullet+}$ complexes display a D_3 and C_2 symmetry, respectively. By performing geometry optimizations in the C_1 symmetry group, we verified that we obtained a higher total energy for both systems. Cartesian coordinates for all atoms in optimized structures of $[Ru(tap)_3]^{\bullet+}$, $[Ru(tap)_2(phen)]^{\bullet+}$, $[Ru(tap)_2(tap\text{-}H)]^{\bullet 2+}$, and $[Ru(tap)(tap\text{-}H)(phen)]^{\bullet 2+}$ are provided in the Supporting Information, Tables 1S−4S.

The same level of theory (B3LYP/6-31G*/Stuttgart) has been adopted in all further in vacuo energy calculations. The electron spin density at the location of the H nuclei as well as the isotropic and anisotropic contributions to the hyperfine interactions were computed for all the DFT wave functions. The total electron spin densities were calculated on a three-dimensional cubic grid with a side length of 20 Å sampled at 150 spacings. The properties of the monoreduced Ru(II) complexes were also estimated in water using the COnductor-like Screening MOdel (COSMO).[31] These calculations were performed at the B3LYP/6-31G*/Stuttgart level of theory using the in vacuo optimized geometries of the complexes.

(14) Closs, G. L. *Adv. Magn. Reson.* **1974**, *7*, 157.
(15) Kaptein, R. *J. Am. Chem. Soc.* **1972**, *94*, 6251.
(16) Munzarova, M. L.; Kaupp, M. *J. Phys. Chem. B* **2001**, *105*, 12644.
(17) Atkins, P.; Friedman, R. *Molecular Quantum Mechanics*, 4th ed.; Oxford University Press: Oxford, 2005.
(18) Saladino, A. C.; Larsen, S. C. *Catal. Today* **2005**, *105*, 122.
(19) Bylaska, E. J.; de Jong, W. A.; Kowalski, K.; Straatsma, T. P.; Valiev, M.; Wang, D.; Aprà, E.; Windus, T. L.; Hirata, S.; Hackler, M. T.; Zhao, Y.; Fan, P.-D.; Harrison, R. J.; Dupuis, M.; Smith, D. M. A.; Nieplocha, J.; Tipparaju, V.; Krishnan, M.; Auer, A. A.; Nooijen, M.; Brown, E.; Cisneros, G.; Fann, G. I.; Früchtl, H.; Garza, J.; Hirao, K.; Kendall, R.; Nichols, J. A.; Tsemekhman, K.; Wolinski, K.; Anchell, J.; Bernholdt, D.; Borowski, P.; Clark, T.; Clerc, D.; Dachsel, H.; Deegan, M.; Dyall, K.; Elwood, D.; Glendening, E.; Gutowski, M.; Hess, A.; Jaffe, J.; Johnson, B.; Ju, J.; Kobayashi, R.; Kutteh, R.; Lin, Z.; Littlefield, R.; Long, X.; Meng, B.; Nakajima, T.; Niu, S.; Pollack, L.; Rosing, M.; Sandrone, G.; Stave, M.; Taylor, H.; Thomas, G.; van Lenthe, J.; Wong, A. Zhang, Z. *NWChem*, 5.0th ed.; Pacific Northwest National Laboratory: Richland, WA, 2006.
(20) Lee, C. T.; Yang, W. T.; Parr, R. G. *Phys Rev B* **1988**, *37*, 785.
(21) Becke, A. D. *J. Chem. Phys.* **1993**, *98*, 5648.
(22) Ditchfield, R.; Hehre, W.; Pople, J. A. *J. Chem. Phys.* **1971**, *54*, 724.
(23) Hariharan, P. C.; Pople, J. A. *Theor. Chim. Acta* **1973**, *28*, 213.
(24) Andrae, D.; Haussermann, U.; Dolg, M.; Stoll, H.; Preuss, H. *Theor. Chim. Acta* **1990**, *77*, 123.
(25) Strassner, T.; Drees, M. *J. Mol. Struct., THEOCHEM* **2004**, *671*, 197.
(26) Drees, M.; Strassner, T. *J. Org. Chem.* **2006**, *71*, 1755.
(27) Alary, F.; Heully, J. L.; Bijeire, L.; Vicendo, P. *Inorg. Chem.* **2007**, *46*, 3154.
(28) Alary, F.; Boggio-Pasqua, M.; Heully, J. L.; Marsden, C. J.; Vicendo, P. *Inorg. Chem.* **2008**, *47*, 5259.
(29) Prechtl, M. H. G.; Holscher, M.; Ben-David, Y.; Theyssen, N.; Milstein, D.; Leitner, W. *Eur. J. Inorg. Chem.* **2008**, 3493.
(30) Boggio-Pasqua, M.; Vicendo, P.; Oubal, M.; Alary, F.; Heully, J. L. *Chem.—Eur. J.* **2009**, *15*, 2759.
(31) Klamt, A.; Schuurmann, G. *J. Chem. Soc., Perkin Trans. 2* **1993**, 799.

The COSMO model is a continuum solvation model implemented in the NWChem program, which determines the solvent reaction field self-consistently with the solute charge distribution described in a quantum mechanical framework. In this model the water solvent (dielectric constant $\varepsilon = 78.4$) is mimicked by a polarizable continuum surrounding a cavity having the shape and dimension of the solute molecule. Interlocking spheres associated with each atom describe the cavity. For the atomic radii, we used the default values, that is, van der Waals radii.

Because of the large size of the investigated complexes, our computations were performed using the 6-31G* basis set for the C, N, and H atoms which includes a quality double-ζ augmented with polarization functions. Although larger basis sets, such as triple-ζ basis sets, have been widely used for the calculation of hyperfine coupling constants of isolated atoms, they involve a highly demanding computational time and, as a consequence, their application is restricted to small and medium size systems.[32,33] For both $[Ru(tap)_3]^{\bullet+}$, $[Ru(tap)_2(phen)]^{\bullet+}$ complexes, the Fermi-contact contribution to the hyperfine coupling constant (A_{iso}) calculated in water with the medium-size basis 6-31G* have been compared to the corresponding values obtained using the large triple-ζ Ahlrichs-VTZ[34] basis set. The Supporting Information, Table 5S contains the results of the calculations. We observe that the Ahlrichs-VTZ basis set influences the Fermi-contact terms only slightly (less than 0.14 gauss). The medium-size basis 6-31G* gives reasonable values of the hyperfine parameters, which, as will be shown below, are in agreement with the experimental results, with moderate computational cost.

Results and Discussion

The C_{2v} symmetry of the tap ligand implies the equivalence of tap H-2 and H-7, H-3 and H-6, as well as H-9 and H-10 (Chart 1). Similarly, the symmetry of the phen ligand implies the equivalence of phen H-2 and H-9, H-3 and H-8, H-4 and H-7 as well as H-5 and H-6. In the ^{1}H NMR spectrum of $[Ru(tap)_3]^{2+}$, three distinctive signals are observed for the three pairs tap H-2,7, H-3,6, and H-9,10 indicating that the three tap ligands are equivalent. For the phen ligand of $[Ru(tap)_2(phen)]^{2+}$, four ^{1}H NMR signals are detected pointing out the equivalence of the H atoms within the pairs phen H-2,9, H-3,8, H-4,7, and H-5,6. For the tap ligands in $[Ru(tap)_2(phen)]^{2+}$, five ^{1}H NMR signals are observed: tap H-2, H-7, H-3, H-6 give rise to distinctive signals while the signals of tap H-9 and H-10 are not resolved, even at high magnetic field.[7] This shows that both tap ligands are analogous, but the equivalence of the H within each pair is not preserved. Indeed, tap H-2, H-3, and H-10 in $[Ru(tap)_2(phen)]^{2+}$ are actually located by the side of the phen ligand while tap H-6, H-7 and H-9 are by the side of the other tap ligand. As mentioned above, ^{1}H photo-CIDNP was observed for the tap ligands, but no significant effect has been measured for the phen ligand of $[Ru(tap)_2(phen)]^{2+}$.[7] For both $[Ru(tap)_3]^{2+}$ and $[Ru(tap)_2(phen)]^{2+}$, the major photo-CIDNP enhancements range between 40 and 60% of the equilibrium signal intensity (measured at 14.1 T and 298 K), and they are observed for the ^{1}H at positions 2 and 7. The photo-CIDNP enhancements of the other ^{1}H NMR signals of the tap ligands were estimated to be lower than 15%, that is, at least three to four times weaker than the enhancements observed for tap H-2 and H-7.

The photo-CIDNP results, for both $[Ru(tap)_3]^{2+}$ and $[Ru(tap)_2(phen)]^{2+}$, suggest a polarization pattern corresponding to a high unpaired electron density in the vicinity of tap H-2 and H-7. To visualize this, we first calculated the electron spin density for the unprotonated and protonated monoreduced complexes. The results obtained in water for $[Ru(tap)_3]^{\bullet+}$, $[Ru(tap)_2(phen)]^{\bullet+}$, $[Ru(tap)_2(tap\text{-}H)]^{\bullet2+}$, and $[Ru(tap)(tap\text{-}H)(phen)]^{\bullet2+}$, both protonated at N-1 and N-8, are shown in Figures 1a−f, respectively. The corresponding results obtained in vacuo are given in the Supporting Information, Figure 1S. For the unprotonated complexes (Figures 1a and 1b), the spin density is primarily found on the tap ligands and predominantly on the N atoms, on the tertiary carbon atoms C-2 and C-7 as well as, to a lesser extent, on the quaternary carbon atoms C-12 and C-13. Some electron spin density is also found on the Ru atom as a spin polarization effect. The electron spin density of the protonated monoreduced complexes (Figures 1c−f) is found to be dramatically different from the spin density of the corresponding unprotonated complexes and is primarily localized on the tap-H ligand in the vicinity of the protonated non-chelating N atom. For $[Ru(tap)_2(phen)]^{\bullet+}$ and $[Ru(tap)(tap\text{-}H)(phen)]^{\bullet2+}$, no significant spin density is observed on the phen ligand.

It is noteworthy that ruthenium-complex radicals have proved difficult to detect by time-resolved EPR (Electron Paramagnetic Resonance) spectroscopy, and that the experimental hyperfine coupling constants are not available.[35−37] However, the Fermi-contact contribution to the hyperfine coupling constant (A_{iso}) is directly proportional to the electron spin density at the position of the H nuclei and therefore can be used directly as a quantitative theoretical parameter related to the measured photo-CIDNP enhancement.[16,17] Table 1 presents the A_{iso} values calculated for $[Ru(tap)_3]^{\bullet+}$ and $[Ru(tap)_2(phen)]^{\bullet+}$ in vacuo and in water. The ^{1}H NMR signals of tap H-9 and tap H-10 in $[Ru(tap)_2(phen)]^{2+}$ are not resolved and, therefore, the average values of the ^{1}H Fermi-contact term are given in parentheses. The calculations in vacuo and in water give very similar values; the main difference appears for tap H-3 of $[Ru(tap)_2(phen)]^{\bullet+}$ with a change of sign between the in vacuo and solvent values. For both complexes, the larger Fermi-contact terms (in absolute value) are computed for the H nuclei at positions 2 and 7 in agreement with the major photo-CIDNP enhancements observed for these atoms.[7] The DFT results are also consistent with the detection of weak photo-CIDNP enhancements for tap H-3,6 and H-9,10. For $[Ru(tap)_2(phen)]^{\bullet+}$, negligible Fermi-contact terms are computed for the H nuclei of the phen ligand for which no ^{1}H photo-CIDNP enhancement was detected.

While the calculated A_{iso} data are in full agreement with the reported steady-state ^{1}H photo-CIDNP experimental results,[7] it is worth considering the possible impact of paramagnetic relaxation. Indeed, steady-state photo-CIDNP enhancements are mainly the result of incomplete cancellation of so-called geminate and escape polarizations.[7−10] Geminate polarizations are carried by the diamagnetic recombination

(32) Eriksson, L. A.; Malkina, O. L.; Malkin, V. G.; Salahub, D. R. *J. Chem. Phys.* **1994**, *100*, 5066.
(33) Fangstrom, T.; Lunell, S.; Engels, B.; Eriksson, L. A.; Shiotani, M.; Komaguchi, K. *J. Chem. Phys.* **1997**, *107*, 297.
(34) Schafer, A.; Horn, H.; Ahlrichs, R. *J. Chem. Phys.* **1992**, *97*, 2571.
(35) Gex, J. N.; Dearmond, M. K.; Hanck, K. W. *J. Phys. Chem.* **1987**, *91*, 251.
(36) Kaim, W.; Ernst, S.; Kasack, V. *J. Am. Chem. Soc.* **1990**, *112*, 173.
(37) van Slageren, J.; Martino, D. M.; Kleverlaan, C. J.; Bussandri, A. P.; van Willigen, H.; Stufkens, D. J. *J. Phys. Chem. A* **2000**, *104*, 5969.

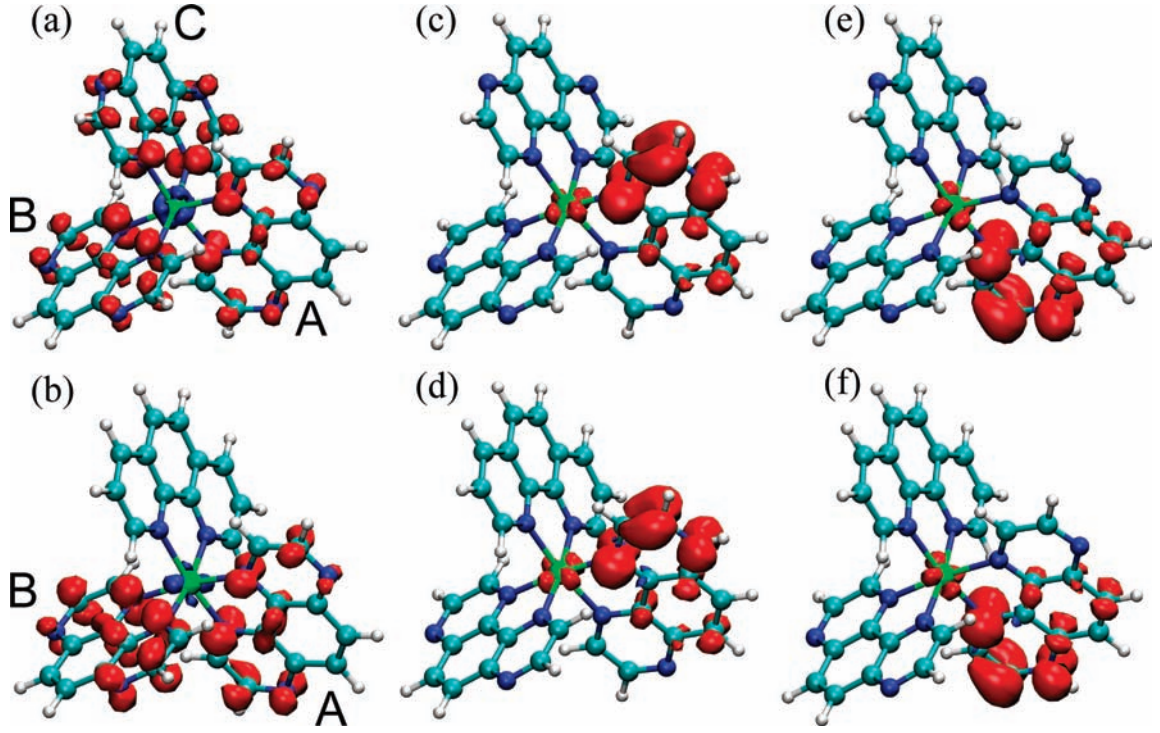

Figure 1. Electron spin density of the unprotonated and protonated monoreduced Ru(II) complexes in water. (a) $[Ru(tap)_3]^{\bullet+}$, (b) $[Ru(tap)_2(phen)]^{\bullet+}$, (c) $[Ru(tap)_2(tap\text{-}H)]^{\bullet 2+}$ protonated at N-1, (d) $[Ru(tap)(tap\text{-}H)(phen)]^{\bullet 2+}$ protonated at N-1, (e) $[Ru(tap)_2(tap\text{-}H)]^{\bullet 2+}$ protonated at N-8, and (f) $[Ru(tap)(tap\text{-}H)(phen)]^{\bullet 2+}$ protonated at N-8. Ru, C, N, and H atoms are colored in green, light blue, dark blue, and white, respectively. The electron spin densities calculated are plotted with constant density contours of +0.003 (red) and −0.003 (blue). Tap ligands are labeled as A, B, or C in (a) and (b).

Table 1. ^{1}H Fermi-Contact Terms (A_{iso} in gauss) and Paramagnetic Relaxation Factors ($Ax^2 + 3Rh^2$ in gauss^2) Calculated in Vacuo and in Water for (a) $[Ru(tap)_3]^{\bullet+}$ and (b) $[Ru(tap)_2(phen)]^{\bullet+}$ [a]

		in vacuo		in water	
		A_{iso}	$Ax^2 + 3Rh^2$	A_{iso}	$Ax^2 + 3Rh^2$
(a)	tap H-2,7	−1.37	7.82	−1.57	9.64
	tap H-3,6	−0.28	1.82	−0.18	1.83
	tap H-9,10	0.06	0.40	0.06	0.39
(b)	tap H-2	−2.04	17.00	−2.36	21.52
	tap H-7	−2.00	16.87	−2.36	22.56
	tap H-3	−0.17	1.93	0.11	1.75
	tap H-6	−0.45	4.80	−0.40	5.31
	tap H-9	0.00 (0.07)	0.80	−0.07 (0.07)	0.89
	tap H-10	0.13	0.60	0.20	0.57
	phen H-2,9	−0.05	2.27	−0.01	2.69
	phen H-3,8	−0.07	0.27	−0.01	0.23
	phen H-4,7	−0.19	0.41	−0.04	0.13
	phen H-5,6	0.01	0.08	0.01	0.06

[a] The ^{1}H NMR signals of tap H-9 and tap H-10 in $[Ru(tap)_2(phen)]^{2+}$ are not resolved and, therefore, the average value of the ^{1}H Fermi-contact term is given in parentheses.

products originating from the primary radical pairs (i.e., the radical pairs generated by the reductive quenching of the excited complexes); their magnitude depends on the isotropic Fermi-contact terms (A_{iso}) as discussed above. Escape polarizations, which are opposite in sign, are first carried by the free radicals originating from dissociation of the primary radical pairs. Initially, escape polarizations are of the same magnitude as the geminate polarizations but longitudinal paramagnetic relaxation brings the nuclear spin state distribution back to equilibrium. Subsequent radical recombination, which usually takes place on the microsecond timescale or slower, also yields the diamagnetic products, and these may carry some residual escape polarizations. The extent of cancellation thus depends on the longitudinal paramagnetic relaxation during the lifetime of the free radicals (the lifetime of the free radicals carrying nuclear spin polarizations). The longitudinal paramagnetic relaxation time depends on the anisotropic part of the electron−nucleus dipolar interaction and is inversely proportional to the paramagnetic relaxation factor ($Ax^2 + 3Rh^2$), where Ax and Rh are the axiality and rhombicity of the anisotropic part of the hyperfine interaction tensor, respectively, defined as[38] $Ax = 2A_{zz} - (A_{xx}+A_{yy})$ and $Rh = A_{yy} - A_{xx}$. Cancellation effects take place if the lifetime of the polarized free radicals is shorter or not much longer than the paramagnetic relaxation time of the nuclear spins. Slow relaxation (a small value of the paramagnetic relaxation factor), and short lifetime increase the cancellation and lead to smaller steady-state photo-CIDNP enhancements.

The ^{1}H paramagnetic relaxation factors ($Ax^2 + 3Rh^2$) calculated for $[Ru(tap)_3]^{\bullet+}$ and $[Ru(tap)_2(phen)]^{\bullet+}$ are given in Table 1. The components of the anisotropic hyperfine interaction tensors are provided in the Supporting Information, Table 6S. A significant paramagnetic relaxation factor is obtained for phen H-2,9 which are the closest phen protons to a tap ligand. The paramagnetic relaxation factors are found to be large for all the ^{1}H that show large Fermi-contact terms. Accordingly, the ordering of the photo-CIDNP enhancements predicted by the A_{iso} values (tap H-2,7 ≫ tap H-3,6 > tap H-9,10) is not expected to change if cancellation effects occur.

The A_{iso} values estimated for the tap-H and tap ligands of the protonated radical species $[Ru(tap)_2(tap\text{-}H)]^{\bullet 2+}$ and

(38) Kuprov, I.; Craggs, T. D.; Jackson, S. E.; Hore, P. J. *J. Am. Chem. Soc.* **2007**, *129*, 9004.

Table 2. ^{1}H Fermi-Contact Terms (A_{iso} in gauss) Calculated in Water for the tap and tap-H Ligands of the Protonated Mono-Reduced Complexes $[Ru(tap)_2(tap\text{-}H)]^{\bullet 2+}$ and $[Ru(tap)(tap\text{-}H)(phen)]^{\bullet 2+}$ [a]

	$[Ru(tap)_2(tap\text{-}H)]^{\bullet 2+}$				$[Ru(tap)(tap\text{-}H)(phen)]^{\bullet 2+}$			
	tap-H	tap B	tap C	average[b]	tap-H	tap B	average[b]	
tap H-2	−6.47	−0.01	0.05		−6.53	−0.02	−3.27	−1.78
	-0.60	*0.01*	*-0.02*	−1.17	*-0.56*	*-0.01*	*-0.28*	
tap H-7	−0.63	0.01	−0.02		−0.57	0.05	−0.26	−1.74
	-6.45	*-0.01*	*0.05*		*-6.46*	*0.01*	*-3.23*	
tap H-3	−1.25	0.00	−0.01		−1.10	−0.04	−0.57	−0.31
	-0.04	*0.01*	*-0.04*	−0.22	*-0.09*	*0.01*	*-0.04*	
tap H-6	−0.04	0.00	−0.04		−0.09	−0.01	−0.05	−0.31
	-1.21	*0.00*	*-0.01*		*-1.15*	*0.00*	*-0.58*	
tap H-9	−1.67	0.00	0.00		−1.75	0.00	−0.88	−0.56[c]
	-0.51	*0.00*	*0.00*	−0.37	*-0.48*	*0.00*	*-0.24*	
tap H-10	−0.53	0.00	0.00		−0.50	0.00	−0.25	−0.56[c]
	-1.69	*0.00*	*0.00*		*-1.76*	*0.00*	*-0.88*	
tap H*	−7.77				−7.70			
	−7.78				*−7.73*			

[a] The values obtained for the N-1 (normal text) and N-8 (italics) protonation of the tap-H ligand are provided. [b] Data averaged according to the symmetry of the corresponding unprotonated diamagnetic complex observed by NMR spectroscopy. The estimated average values assume identical pK_a for the two non-chelating nitrogen atoms of the tap ligands of $[Ru(tap)_2(phen)]^{\bullet +}$. [c] The ^{1}H NMR signals of tap H-9 and tap H-10 in $[Ru(tap)_2(phen)]^{2+}$ are not resolved.

Table 3. ^{1}H Paramagnetic Relaxation Factors ($Ax^2 + 3Rh^2$, in gauss^2) Calculated in Water for the tap and tap-H Ligands of the Protonated Mono-Reduced Complexes $[Ru(tap)_2(tap\text{-}H)]^{\bullet 2+}$ and $[Ru(tap)(tap\text{-}H)(phen)]^{\bullet 2+}$ [a]

	$[Ru(tap)_2(tap\text{-}H)]^{\bullet 2+}$				$[Ru(tap)(tap\text{-}H)(phen)]^{\bullet 2+}$			
	tap-H	tap B	tap C	average[b]	tap-H	tap B	average[b]	
tap H-2	178.08	0.27	0.54		179.55	0.10	89.83	45.59
	2.65	*0.41*	*0.10*	31.35	*2.42*	*0.27*	*1.34*	
tap H-7	2.76	0.40	0.10		2.46	0.53	1.50	45.20
	177.43	*0.27*	*0.53*		*177.40*	*0.41*	*88.91*	
tap H-3	32.63	1.69	12.79		30.19	0.89	15.54	8.63
	1.75	*2.60*	*0.82*	8.65	*1.76*	*1.68*	*1.72*	
tap H-6	1.75	2.53	0.80		1.78	12.63	7.21	11.93
	32.03	*1.71*	*12.63*		*30.79*	*2.52*	*16.65*	
tap H-9	16.77	0.15	0.05		17.92	0.07	9.00	6.79[c]
	9.08	*0.13*	*0.07*	4.40	*9.01*	*0.15*	*4.58*	
tap H-10	9.02	0.13	0.07		8.99	0.06	4.52	6.80[c]
	17.16	*0.15*	*0.05*		*18.01*	*0.13*	*9.07*	
tap H*	525.29				530.34			
	538.51				*534.39*			

[a] The values obtained for the N-1 (normal text) and N-8 (italics) protonation of the tap-H ligand are provided. [b] Data averaged according to the symmetry of the corresponding unprotonated diamagnetic complex observed by NMR spectroscopy. The estimated average values assume fast protonation−deprotonation equilibrium with respect to both the radical lifetime and the ^{1}H relaxation rates in the radical as well as identical pK_a for the two non-chelating nitrogen atoms of the tap ligands of $[Ru(tap)_2(phen)]^{\bullet +}$. [c] The ^{1}H NMR signals of tap H-9 and tap H-10 in $[Ru(tap)_2(phen)]^{2+}$ are not resolved.

$[Ru(tap)(tap\text{-}H)(phen)]^{\bullet 2+}$ are reported in Table 2. The values obtained for the N-1 and N-8 protonation of the tap-H ligand are provided. All corresponding values calculated in vacuo are given in the Supporting Information, Table 7S. The results for the phen ligand do not change significantly, and the Fermi-contact terms remain negligible (not shown). The A_{iso} values calculated for the unprotonated tap ligands (tap B and tap C in Table 2) are now found to be negligible as well; significant A_{iso} values are found for the protonated tap-H ligand only. However, for comparison with photo-CIDNP results, the A_{iso} values calculated for the tap and tap-H ligands must be averaged over equivalent positions in the diamagnetic unprotonated complex (and over positions giving unresolved ^{1}H NMR signals) since the polarization is detected on these species. The major average A_{iso} values are still observed for the H nuclei at position 2 and 7. Interestingly, the average Fermi-contact term calculated for tap H-9,10 is significantly larger (in absolute value) than the average value for the H nuclei at position 3 or 6. In contrast, for the unprotonated monoreduced complexes (Table 1), the average Fermi-contact term calculated for tap H-9,10 is almost negligible. This observation suggests that time-resolved photo-CIDNP measurements, which allow to directly measure geminate polarizations,[9] might provide information on the protonation state of these complexes. However, in addition to the need of a suitable pulsed laser and an adapted experimental setup, such measurements have lower sensitivity (poorer signal-to-noise ratio) than steady-state experiments

and the enhancements of the tap H-3,6 and tap-H-9,10 are probably too small to be measured with precision. The ^{1}H paramagnetic relaxation factors calculated for the tap-H and tap ligands of the protonated monoreduced complexes are given in Table 3. The corresponding values calculated in vacuo as well as all the components of the anisotropic hyperfine interaction tensors are provided in the Supporting Information, Tables 8S-10S. For the averaging over equivalent positions in the corresponding unprotonated diamagnetic complexes, it was assumed that proton exchange with water molecules is a fast process (i) with respect to the lifetime of the polarized free radicals (i.e., the various nonchelating N atoms of the tap ligands undergo multiple protonation−deprotonation events) and (ii) with respect to the shortest ^{1}H paramagnetic longitudinal relaxation time. In Table 3, the paramagnetic relaxation factors are found to be large for the ^{1}H that show large Fermi-contact terms. Similar to the trend observed for the Fermi-contact terms, with respect to the values for tap H-3 and tap H-6, the paramagnetic relaxation factor for tap H-9,10 is significantly larger in the protonated radicals than in the corresponding unprotonated forms. Accordingly, a larger enhancement for tap H-9,10 is expected in the protonated form. Precise steady-state photo-CIDNP measurements for tap H-9,10 and tap H-3,6 might thus prove to be informative with respect to the protonation state of transient monoreduced Ru(II) complexes comprising of tap ligands.

Conclusion

In conclusion, the present DFT study shows that steady-state ^{1}H photo-CIDNP enhancements arising from the photoreaction of Ru(II) complexes agree with the unpaired electron density in the transient ruthenium-complex radicals. The calculations predict that the protonation of a tap ligand in the monoreduced complex should significantly affect the ^{1}H photo-CIDNP enhancements of tap H-9,10. Accordingly, high precision steady-state photo-CIDNP experiments, or time-resolved measurements if feasible, and comparison of the enhancements observed for positions 3,6 and 9,10 might provide information on the photoreaction mechanism. This result is particularly important in the interpretation of the photoreactivity of Ru(II) complexes with biomolecules for which a proton transfer has been proposed.[39] In the future, combined photo-CIDNP experiments and DFT calculations are expected to offer unprecedented opportunities for characterizing transient monoreduced Ru(II) complexes. The agreement between the theoretical and experimental results reported in this work shows that the use of a polarizable continuum solvation model, such as COSMO, to take into account the solvent effects is a very good alternative to explicit solvent representation because the COSMO model partly includes solute polarization through the polarization charge of the continuum, leading to qualitatively accurate values of spin density with lower computational time. However, it would be worthwhile to extend our study to include the explicit modeling of the solvent molecules. Indeed, consideration of the hydrogen bonding may be expected to induce some redistribution of the spin-densities of the monoreduced Ru(II) complexes allowing for a more quantitative treatment of the photoreaction of these complexes.

Acknowledgment. This work was supported by the Communauté Française de Belgique (ARC) and the F. R.S.-FNRS (Fonds National de la Recherche Scientifique de Belgique). E.C. is Postdoctoral Researcher at the FNRS. M.L., E.M., and L.F. thank the F.R.S.-FNRS for financial support (FRFC 2.4.642.08 and 2.4.519.08). L.F. thanks the "Regione Autonoma della Sardegna" for financial support.

Supporting Information Available: List of Cartesian coordinates of optimized DFT structures of $[Ru(tap)_3]^{\bullet+}$, $[Ru(tap)_2(tap\text{-}H)]^{\bullet2+}$, $[Ru(tap)_2(phen)]^{\bullet+}$ and $[Ru(tap)(tap\text{-}H)(phen)]^{\bullet2+}$. Figure 1S for the electron spin density in vacuo of $[Ru(tap)_3]^{\bullet+}$, $[Ru(tap)_2(tap\text{-}H)]^{\bullet2+}$, $[Ru(tap)_2(phen)]^{\bullet+}$ and $[Ru(tap)(tap\text{-}H)(phen)]^{\bullet2+}$. Table 5S for the A_{iso} values in water of $[Ru(tap)_3]^{\bullet+}$ and $[Ru(tap)_2(phen)]^{\bullet+}$ estimated using 6-31G* and Ahlrichs-VTZ basis sets. Table 6S for the components of the anisotropic hyperfine interaction tensors in vacuo and in water for $[Ru(tap)_3]^{\bullet+}$ and $[Ru(tap)_2(phen)]^{\bullet+}$. Tables 7S-8S for the A_{iso} and $Ax^2 + 3Rh^2$ values in vacuo of $[Ru(tap)_2(tap\text{-}H)]^{\bullet2+}$ and $[Ru(tap)(tap\text{-}H)(phen)]^{\bullet2+}$. Tables 9S-10S for the components of the anisotropic hyperfine interaction tensors in vacuo and in water for $[Ru(tap)_2(tap\text{-}H)]^{\bullet2+}$ and $[Ru(tap)(tap\text{-}H)(phen)]^{\bullet2+}$. Tables 11S-14S for the Mulliken charges of the monoreduced Ru(II) complexes. This material is available free of charge via the Internet at http://pubs.acs.org.

(39) Elias, B.; Creely, C.; Doorley, G. W.; Feeney, M. M.; Moucheron, C.; Kirsch-DeMesmaeker, A.; Dyer, J.; Grills, D. C.; George, M. W.; Matousek, P.; Parker, A. W.; Towrie, M.; Kelly, J. M. *Chem.—Eur. J.* **2008**, *14*, 369.